J Mol Model (2012) 18:3969–3980
DOI 10.1007/s00894-012-1391-6

ORIGINAL PAPER

Chemical reactivity analysis of deoxyribonucleosides and deoxyribonucleoside analogues (NRTIs): a first-principles density functional approach

Vipin Kumar · Shyam Kishor · Lavanya M. Ramaniah

Received: 4 January 2012 / Accepted: 21 February 2012 / Published online: 21 March 2012

Abstract The structures, energetics, as well as several important chemical parameters, of antiretroviral drugs - nucleoside reverse transcriptase inhibitors (NRTIs) - and natural deoxyribonucleosides in both neutral, and positively and negatively charged states, are investigated. These studies are carried out within the frame work of first-principles density-functional theory (DFT), using the Becke-Lee-Yang-Parr (BLYP) generalized gradient corrections to the local spin density approximation exchange and correlation energy, norm-conserving pseudopotentials and a plane-wave expansion of Kohn-Sham orbitals. Conceptual DFT is used to determine global and local chemical reactivity parameters. Our results are in good agreement with the best available experiments to date. The variation in the bond lengths and bond angles on cation formation indicates that the electron is lost from the base part of these molecules. Further, the presence of the deoxyribose sugar moiety lowers their ionization potential and increases their electron affinity, in comparison to the isolated DNA base. The effectiveness of the drug action in terminating the viral DNA chain, is explained using the global reactivity parameters, by comparing the reactivities of the drug molecules with those of the competing deoxyribonucleosides. The widely followed clinical practice, of avoiding the simultaneous administration of certain drugs, is also explained from the hardness and softness parameters. For most of the drug molecules, our study validates the generally accepted wisdom, that monophosphorylation is the crucial reaction step in the phosphorylation reaction in DNA nucleotide synthesis.

Keywords Chemical reactivity · Density functional theory · Deoxyribonucleosides · Fukui function · NRTIs

Electronic supplementary material The online version of this article (doi:10.1007/s00894-012-1391-6) contains supplementary material, which is available to authorized users.

V. Kumar (✉) · S. Kishor
Department of Chemistry, J. V. College,
Baraut, Uttar Pradesh 250611, India
e-mail: vipin.chemia@gmail.com

L. M. Ramaniah
High Pressure and Synchrotron Radiation Physics Division,
Bhabha Atomic Research Centre,
Trombay, Mumbai 400085, India

Introduction

Deoxyribonucleosides are glycosylamines consisting of a nucleobase (pyrimidine or purine) bound to a deoxyribose sugar via a beta-glycosidic linkage. The purine-based deoxyribonucleosides are deoxyadenosine (dA) and deoxyguanosine (dG), while the pyrimidine-based deoxyribonucleosides are deoxythymidine(dT) and deoxycytidine(dC). These deoxyribonucleosides, on phosphorylation at their sugar primary alcohol (CH_2OH) group, get converted to the DNA molecule building blocks, i.e., deoxyribonucleotides. In medicine, several deoxyribonucleoside analogues are used as antiviral drugs and are among the most widely researched classes of drugs. Nucleoside reverse transcriptase inhibitors (NRTIs) were the first class of drugs that were introduced as antiretroviral agents for the treatment of human HIV infection. NRTIs block the enzymatic function of reverse transcriptase (a viral DNA polymerase enzyme) and prevent completion of synthesis of the double-stranded viral DNA, thus preventing HIV from multiplying. Examples of NRTIs currently approved [1] for the treatment of HIV infection include deoxycytidine analogues (Lamivudine (3TC), Zalcitabine (ddC) and Emtricitabine (FTC)), deoxythymidine analogues (Stavudine (d4T) and Zidovudine (AZT)), deoxyadenosine analogue (Didanosine (ddI)) and deoxyguanosine analogue (Abacavir (ABC)).

As the NRTIs are analogues of the naturally occurring deoxyribonucleosides needed to synthesize the viral DNA, hence they compete with the natural deoxyribonucleotides for phosphorylation and consequent incorporation into the growing viral DNA chain. Further, unlike the natural deoxyribonucleotides, NRTIs lack a 3′-hydroxyl group on the deoxyribose moiety. As a result, following incorporation of an NRTI, the next incoming deoxyribonucleotide cannot form the next 5′–3′ phosphodiester bond needed to extend the DNA chain. Thus, when an NRTI is incorporated, viral DNA synthesis is halted, a process known as chain termination [2–4]. For NRTIs to be effective against HIV, they must be taken up by the host cell and then phosphorylated by cellular enzymes to convert them to their active triphosphate analogues. Phosphorylation occurs in three steps. The first step involves the formation of monophosphate, which then gets converted to diphosphate and finally to the active triphosphate. The efficiency and regulation of these pathways vary and have not been fully characterized for all the agents.

In recent years, there have been several experimental and theoretical studies of biological molecules, such as DNA bases, and even a few on deoxyribonucleosides and NRTIs. Molecular beams provide the means to determine experimental gas phase ionization potential and electron affinities [5, 6, 8]. The first gas phase adiabatic ionization potential (IP) of purine and pyrimidine bases were measured by photoionization mass spectrometry [5]. The adiabatic electron affinity of the nucleic acid bases has been determined by negative ion photoelectron spectroscopy and by collision with laser-excited Rydberg atoms [6]. The vertical IP of DNA bases has been calculated at the B3LYP/6-31++G(d,p) [7], as well as HF/6-31+G(d), MP2, OVGF-MP2 and PMP2 levels. Ultraviolet photoelectron spectroscopy has been employed to obtain the vertical ionization potentials of volatile nucleoside models [8]. The vertical and adiabatic ionization potentials of purine deoxyribonucleosides have been calculated at the PMP2/aug-cc-pvdz level [9]. The electron affinities of the deoxyribonucleosides have been evaluated using the B3LYP hybrid Hartree Fock/ DFT functional with the DZP++ basis set [10].

The few studies of the NRTIs include the determination of the solvent effects on the molecular structure and energetics of the most stable conformers of d4T, using MP2 and DFT methods [11]. Conformational properties and the energy barriers between the *anti* and the *syn* configurations of 3TC, ddC, AZT and d4T molecules have been examined using DFT [12]. The 3TC conformers have been identified by Raman scattering measurements and quantum chemical DFT calculations [13]. The effects of intramolecular H-bonds have been determined through a topological analysis of the Hartree-Fock electronic charge density in derivatives of 3TC [14] and AZT [15]. Molecular dynamics simulations of complexes of HIV-1 reverse transcriptase with the substrate and the antiretrovirals AZT and d4T have been conducted [16]. However, systematic studies and in particular, detailed analyses of various properties, of these chemically and biologically important molecules, are yet to appear.

In this paper, we present a comparative study of the ground state energies, structures, ionization potentials, electron affinities and DFT-based global and local chemical reactivity descriptors of the antiretroviral drugs - nucleoside reverse transcriptase inhibitors (NRTIs), viz., ddC, 3TC, FTC, d4T, AZT, ddI and ABC - and their respective deoxyribonucleosides. The structural properties, the ionization potentials and electron affinities of the drugs and deoxyribonucleosides are also compared with those of the DNA bases. Using global reactivity parameters, the reactivities of the NRTIs toward mono-phosphorylation is compared with that of their deoxyribonucleosides. These reactivities are further evaluated using local reactivity parameters, specifically, the condensed-to-oxygen-atom Fukui function f_k^- on the primary hydroxyl group present in the sugar moiety.

In the next section, the theoretical framework and the computational method and details are briefly outlined. The results of our calculations are presented and discussed in Results and discussion section. The summary and conclusions of the paper are given in Conclusions section.

Theory and computational details

Theory

As the number of electrons (N) in a many electron system (such as an atom, ion or molecule) and the external potential $v(\vec{r})$ fix its Hamiltonian, hence all the properties of the system may be obtained by the appropriate variations of N and $v(\vec{r})$. This approach to analyzing chemical behavior, termed "conceptual DFT" [17–22], has been quite successful in providing a theoretical basis for popular qualitative chemical descriptors such as electronegativity (χ), chemical potential (μ), chemical hardness (η), chemical softness (S) and electrophilicity index (ω), which describe the reactivity of the molecule as a whole [23] and are thus known as the global reactivity parameters.

The absolute electronegativity (χ) [24, 25], chemical potential (μ) [26], chemical hardness (η) [27] and chemical softness (S) [28] may be defined as

$$\chi = -\mu = -\left(\frac{\partial \mathrm{E}}{\partial \mathrm{N}}\right)_{v(\vec{r})} = \frac{(IP + EA)}{2} \quad (1)$$

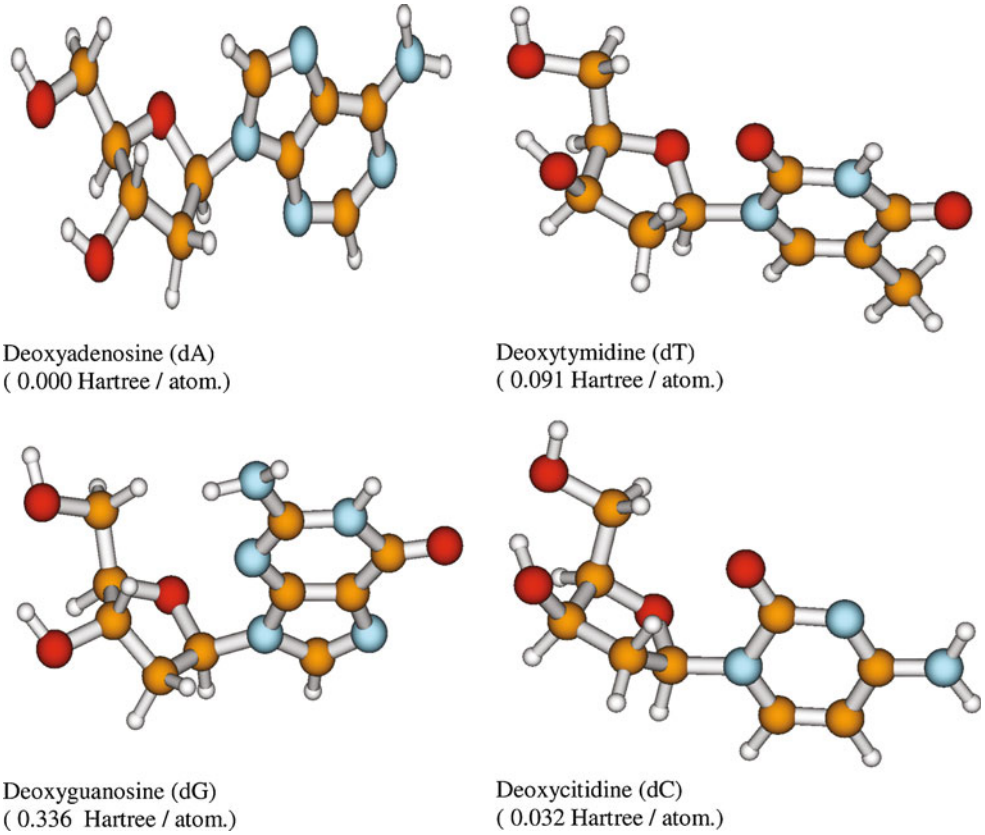

Fig. 1 Optimized structures of deoxyribonucleoside molecules

$$\eta = \frac{1}{2}\left(\frac{\partial^2 \mathrm{E}}{\partial \mathrm{N}^2}\right)_{v(\vec{r})} = \frac{1}{2}\left(\frac{\partial \mu}{\partial \mathrm{N}}\right)_{v(\vec{r})} = \frac{(IP - EA)}{2} \tag{2}$$

$$S = \frac{1}{2\eta} \tag{3}$$

where E(N) is the electronic energy of the N-electron system.

The ionization potential(IP) and the electron affinity (EA) may be expressed, using the finite difference approximation, as :

$$IP = E(N-1) - E(N) \text{ and } EA = \mathrm{E}(N) - E(N+1) \tag{4}$$

The global electrophilicity index (ω) [29, 30], given by

$$\omega = \frac{\mu^2}{2\eta} \tag{5}$$

quantifies the tendency of a molecule to accept electrons from a generic donor.

In various chemical and biological reactions of drugs with DNA or other molecules, the characterization of active sites is an important task. The identification of the active sites in a molecule is made by the calculation of Fukui functions. The condensed Fukui functions as proposed by Yang and Mortier [31], considering a finite difference method, can be obtained using the Mulliken population analysis (MPA) scheme as:

$$f_k^{+} = q_k(N+1) - q_k(N) \quad \text{(for nucleophilic attack)} \tag{6}$$

$$f_k^{-} = q_k(N) - q_k(N-1) \quad \text{(for electrophilic attack)} \tag{7}$$

$$f_k^{0} = \frac{q_k(N+1) - q_k(N-1)}{2} \quad \text{(for radical attack)} \tag{8}$$

where q_k is the electronic population of atom k in a molecule. A large value of f_k^{+}, f_k^{-} or f_k^{0} at any site would indicate the probability of that respective (nucleophilic, electrophilic or radical) attack at that site, which would correspond to a large change in chemical potential. All the local parameters can be related to the global parameters through the Fukui functions; thus, for example, the local softness $(s(\vec{r}))$ is related to the global softness (S) through the relation,

$$s(\vec{r}) = f(\vec{r})S \tag{9}$$

Computational details

We work within the density functional theory (DFT) approach [32, 33, 34], including the generalized gradient

corrections (GGA) to the local spin density approximation (LSDA) [35]. Valence electrons are treated explicitly and their wavefunctions are expanded in a plane wave basis set with an energy cut-off of 70 Ry, while core-valence interactions are described by norm-conserving pseudopotentials [36], which have been carefully tested for both convergence and transferability [37–41].

In each case, the molecule is placed in an orthorhombic simulation cell, whose side ranges in length from 7.5 - 34 Å. The large size of the cell, chosen to be at least twice the largest dimension of the molecule, ensures a sufficient reduction of finite-size effects. In order to avoid the spurious interactions with the images of the system in neighboring simulation cells, which occur with the use of periodic boundary conditions, we adopt an isolated cell approach following the scheme of Barnett and Landmann [42] and refined by Tuckerman [43, 44]. For ionized molecules, a uniformly charged background compensates the molecule charge.

For the sake of self-consistency within the density functional theory used, as well as to optimize the trial structure constructed, geometry relaxations are carried out on a given molecule. In this way, the initial guessed system goes to the nearest local minimum of the potential energy surface, representing a stable molecular configuration.

The geometry of the molecule is fully relaxed via direct inversion in iterative subspace (DIIS) [45], as implemented in the CPMD code [46, 47], until the largest component of the ionic forces attains a value $<5\times10^{-4}$ a.u. For these calculations, we use the GGA due to Becke and Lee, Yang and Parr [48, 49] (BLYP), for the exchange and correlation functionals, respectively. The ionization potential and electron affinity of the molecule are then investigated and their vertical and adiabatic values are obtained. Finally, the DFT-based global and local chemical reactivity descriptors of interest defined earlier are calculated.

Results and discussion

Structural properties

The fully optimized structures of the deoxyribonucleosides and their corresponding analogues (NRTIs) are shown in Figs. 1 and 2 respectively, with the total energy per atom of each molecule with reference to that of the lowest energy molecule (dA and FTC, respectively) indicated in the captions. The figures (Figs. 1–11), provided in the Supplementary data, specifically indicate the variation of the bond-lengths in the cations and anions of the NRTIs, as compared to the neutral molecules. In addition, the bond lengths and bond angles of those nucleoside and NRTIs, whose experimental and theoretical values are available in the literature, are also given (Tables I–VIII), in the Supplementary data. To the best of our knowledge, no theoretical and experimental data is available for the other molecules. Our results are in very good agreement with the available experimental data, giving confidence in the ability of DFT to accurately describe this class of systems. Our computed bond lengths of the important glycosidic bond (which joins the purine or pyramidine base to the deoxyribose in deoxyribonucleosides or their analogues) are in better agreement with the experimental [50–56] values than earlier theoretical calculations [10].

An examination of the geometry-optimized structures of the deoxyribonucleosides and their analogues, shows that the geometrical variation from the neutral structure is more in the cations than in the anions. The exception is AZT, the dT analogue, which has an affinity for an electron due to the presence of positive charge on the central nitrogen atom of the N=N=N- (azide group). Consequently, there is a large variation (0.06 Å and 0.11 Å) in the N=N=N bond lengths in the sugar moiety. The N-N-N bond angle also undergoes a large variation from 172.48° in the neutral to 132.48° in the anion, indicating a change in hybridization around the central nitrogen atom from sp to sp^2, upon acquiring an electron. For the pyrimidine-based deoxyribonucleosides (dT, dC) and their analogues, the root mean square (RMS) deviation in bond length (Table 1) on cation formation is dC (0.023 Å)>FTC (0.020 Å)>d4T (0.018 Å)>ddC (0.017 Å)>dT (0.016 Å)> AZT (0.013 Å), whereas on anion formation it is AZT (0.023 Å) >>3TC=FTC (0.010 Å)>dC (0.008 Å)>d4T (0.007 Å)>ddC (0.006 Å). For the purine-based deoxyribonucleosides (dA, dG) and their analogues, the RMS deviation in bond length on cation formation is dG (0.020 Å)>dA=ddI (0.017 Å)>ABC (0.015 Å); and on anion formation, it is dA (0.010 Å)>ddI (0.006 Å)>dG (0.004 Å)>ABC (≈ 0.0). Among the deoxyribonucleosides, the smallest variation in geometry in the anion is found in dG. A similar conclusion was arrived at from earlier theoretical calculations using B3LYP/DZP++[10].

The study of the influence of excess charge, upon the formation of a cation or an anion (which may occur due to the interaction with an oxidizing or reducing agents or from exposure to radiation), on different specific bonds gives clues to the mechanism of bond making and bond cleavage. For instance, the glycosidic bond elongates (0.02 - 0.03 Å) in the cation in comparison to the neutral molecule, in the purine-based deoxyribonucleosides and their analogues. Among the cations of pyrimidine-based deoxyribonucleosides and their analogues, elongation is only found in the case of dT and its analogues. There is significant elongation (0.05 Å) in the case of d4T. This implies that exposure to an oxidizing agent or radiation weakens the glycosidic bond and may cause its cleavage in the cation. Another important general trend observed in the anions of all the deoxyribonucleosides and their

Fig. 2 Optimized structures of NRTI drug molecules

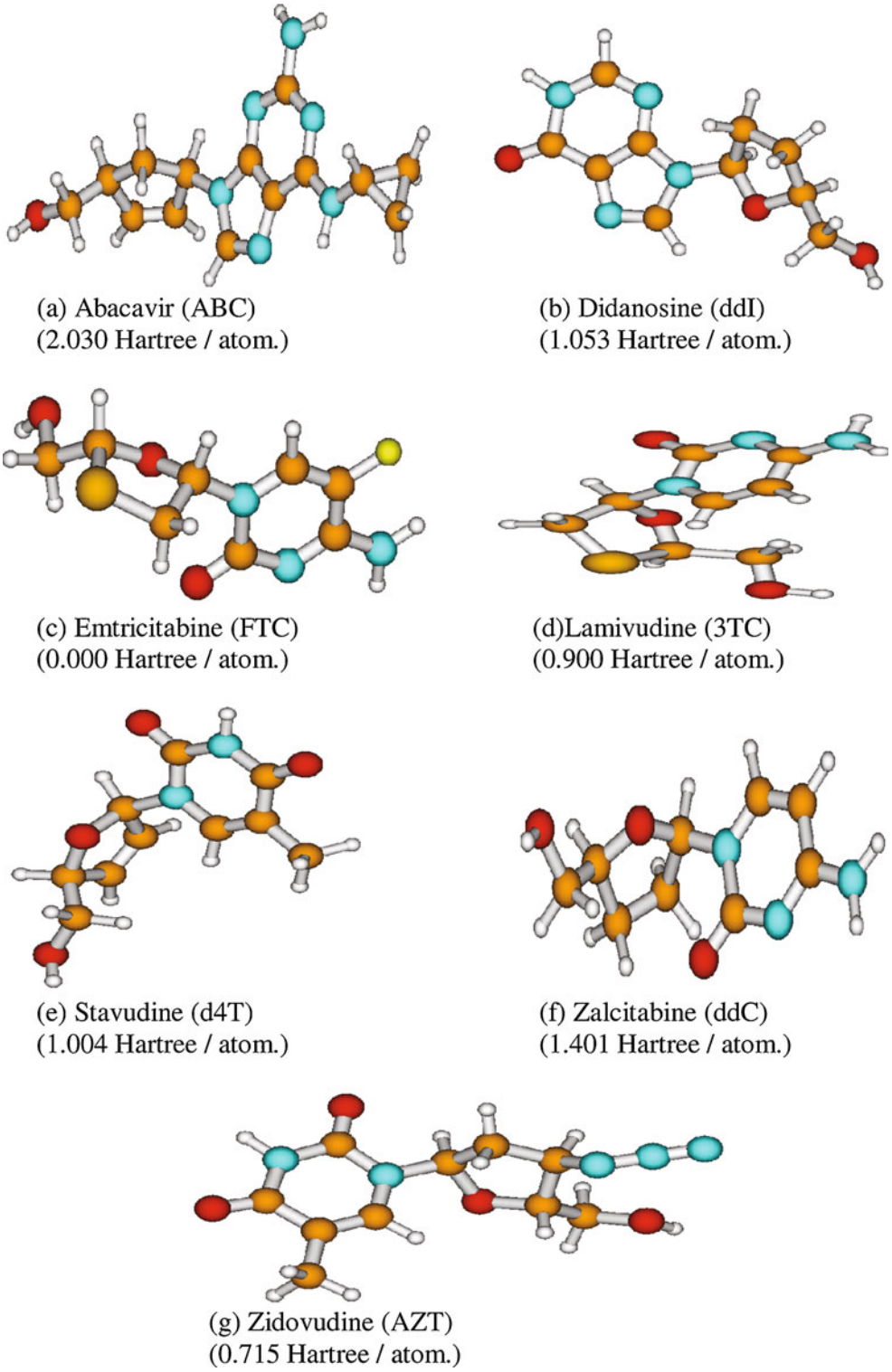

Fig. 3 Schematic diagram of the monophosphorylation reaction

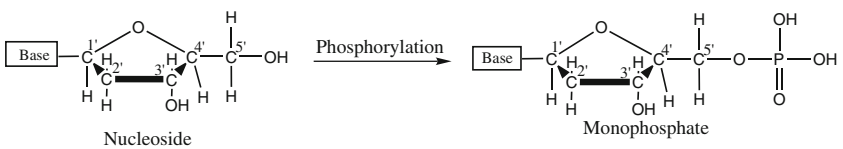

Table 1 Root mean square deviation (RMSD) values of bond lengths (Å) and bond angles(°)

Deoxyribonucleosides/ analogues (NRTIs)	RMSD in bond length		RMSD in bond angle	
	On cation formation	On cation formation	On anion formation	On anion formation
dA	0.017	0.010	0.599	0.230
ddI	0.017	0.006	0.629	0.409
dT	0.016	0.010	1.245	1.070
d4T	0.017	0.007	1.259	0.591
AZT	0.013	0.023	1.258	7.883
dG	0.020	0.004	1.144	0.207
ABC	0.015	0.000	0.969	0.038
dC	0.023	0.008	2.096	0.625
FTC	0.020	0.010	2.008	0.654
3TC	0.014	0.010	1.133	0.532
ddC	0.017	0.006	1.997	0.688

analogues, is that the glycosidic bond shortens compared to their neutral species. A similar trend was observed for deoxyribonucleosides in earlier theoretical calculations using B3LYP/DZP++[10]. There is no significant geometric variation found in the sugar moiety of deoxyribonucleosides and NRTIs after acquiring charge, implying that the excess charge resides on the nucleic acid bases. A similar observation was made earlier from B3LYP/DZP++[10] calculations for the deoxyribonucleosides.

An interesting trend is observed for the pyrimidine nucleoside, dC, and is analogues (3TC, ddC, and FTC), namely, alternate bond elongation (C_4-N_3, C_2-O_2) and bond shortening (N_1-C_2, N_4-C_4, N_3-C_2) in the base on cation formation. This suggests that the loss of an electron triggers extensive delocalization in the base moiety of the molecules. In the case of another pyrimidine nucleoside dT and its analogues (d4T and AZT), the $N_1'-N_6'$ bond in the base elongates significantly by≈0.05 Å. In the case of the purine nucleosides, dA and dG, and their analogues ddI and ABC, on cation formation, there is extensive alternate bond elongation and bond shortening in both rings of the purine base. We note that, this trend in the geometric alteration of the base bonds in the cations of deoxyribonucleosides and NRTIs, indicates that the electron is lost from the bases of the molecules.

Ionization potential and electron affinity

Table 2 gives the values of the ionization potential (IP) and the electron affinity (EA), both vertical and adiabatic, as calculated by us for the DNA bases [59], deoxyribonucleosides and their analogues (NRTIs). The vertical ionization potential (electron affinity) is the difference in total energies of the neutral and positively (negatively) charged molecules, with the molecular geometry having once been optimized in the neutral state. The adiabatic ionization potential (electron affinity) is calculated as the difference in total energies of the relaxed neutral cluster and the relaxed positively (negatively) charged cluster with the same topology.

It is known [57, 58], from the much higher extinction coefficient of the bases as compared to the deoxyribose, that the ionization of the deoxyribonucleosides takes place predominantly at the base moiety. However, the presence of the sugar has a strong effect on the energetics of the ionization of the base. This is reflected in our computed values for the vertical and adiabatic ionization potentials of the deoxyribonucleosides, which are found to be lower than in their corresponding bases [59]. The minimum difference in the vertical ionization potentials is between guanine(G) and dG (0.082 eV), while the maximum difference is between thymine(T) and dT (0.599 eV). The IP difference between adenosine(A) and dA is 0.323 eV, and between cytosine (C) and dC is 0.445 eV.

We find a similar trend for the NRTIs. Our computed values for the vertical and adiabatic ionization potentials of the NRTIs are lower than in their corresponding bases. The maximum difference (0.85 eV) in the vertical IP is between the dG analogue, ABC and guanine, and the minimum difference (0.21 eV) is between adenosine and the dA analogue, ddI. The IP difference between cytosine and the dC analogues ranges between 0.577 eV- 0.688 eV, and between thymine and the dT analogue is 0.738 eV (AZT) and 0.554 eV (d4T). In addition to the above-mentioned features, the computed vertical IPs are useful for evaluating the reactivity descriptors, as mentioned earlier.

The adiabatic ionization potential is found to be lower than the corresponding vertical ionization potential. A similar trend was observed in our earlier study of amino acids [60]. Our result is in accordance with the basic principle that relaxation stabilizes the molecules. The mean relaxation energy difference between the vertical and adiabatic IP for

Table 2 Calculated ionization potentials (IP) (eV), electron affinities (EA) (eV) and global chemical reactivity descriptors for the molecules : electronegativity (χ), chemical potential (μ), chemical hardness (η), chemical softness (S), electrophilicity index (ω) and dipole moment (D.M.). Also given for comparison are the theoretical [10, 71] and experimental [62, 73] values obtained from the literature

DNA bases[59]/ deoxyribonucleosides/ analogues (NRTIs)	Vertical IP (eV)	Adiabatic IP (eV)	Vertical EA (eV)	Adiabatic EA (eV)	ΔEA	$\chi=-\mu$	η	S	ω	D.M. (D)
Adenosine (A)	7.919	7.756	0.410	0.410	0.000	4.165	3.755	0.133	2.307	2.331
B3LYP/DZP++[10]				−0.28						2.510
Exp.[62]				0.75						
Exp.[73]										2.270
Deoxyadenosine (dA)	7.596	7.451	0.520	0.522	0.002	4.058	3.538	0.141	2.322	4.299
B3LYP/DZP++[10]				0.060						2.390
B3LYP/6-31++G(d,p)[71] [syn]	8.190									
B3LYP/6-31++G(d,p)[71] [Anti]	7.860									
Didanosine (ddI)	7.709	7.479	0.501	0.581	0.080	4.105	3.604	0.139	2.338	7.331
Thymine (T)	8.578	8.383	−0.208	0.021	0.229	4.185	4.393	0.114	1.997	4.474
B3LYP/DZP++[10]				0.20						4.590
Exp.[62]				0.65						
Exp.[73]										4.510
Deoxythymidine (dT)	7.979	7.740	0.512	0.585	0.073	4.246	3.734	0.134	2.416	4.318
B3LYP/DZP++[10]				0.440						4.460
B3LYP/6-31++G(d,p)[71] [syn]	8.620									
B3LYP/6-31++G(d,p)[71] [Anti]	8.310									
Stavudine (d4T)	8.024	7.890	0.507	0.528	0.021	4.266	3.759	0.133	2.421	5.567
Zidovudine (AZT)	7.840	7.701	0.542	1.039	0.497	4.191	3.649	0.137	2.406	4.343
Guanine (G)	7.527	7.329	0.492	0.493	0.001	4.010	3.518	0.142	2.283	6.791
Exp.[62]				1.05						
B3LYP/DZP++[10]				−0.07						6.740
Exp.[73]										6.550
Deoxyguanosine (dG)	7.445	7.162	0.430	0.446	0.016	3.938	3.508	0.143	2.218	7.021
B3LYP/DZP++[10]				0.090						
B3LYP/6-31++G(d,p)[71] [syn]	7.950									
B3LYP/6-31++G(d,p)[71] [Anti]	7.570									
Abacavir (ABC)	6.672	6.384	0.569	0.570	0.001	3.621	3.051	0.164	2.148	0.964
Cytosine (C)	8.317	8.219	0.449	0.725	0.276	4.383	3.934	0.127	2.440	6.484
B3LYP/DZP++[10]				0.03						6.790
Exp.[62]				0.60						
Exp.[73]										6.020
Deoxycytidine (dC)	7.872	7.524	0.534	0.565	0.031	4.203	3.669	0.136	2.402	5.898
B3LYP/DZP++[10]		–		0.330						
B3LYP/6-31++G(d,p)[71] [syn]	8.480									
B3LYP/6-31++G(d,p)[71] [Anti]	8.090									
Emtricitabine (FTC)	7.740	7.263	0.619	0.658	0.039	4.179	3.560	0.140	2.453	7.286
Lamivudine (3TC)	7.629	7.458	0.503	0.554	0.051	4.065	3.562	0.140	2.320	5.774
Zalcitabine (ddC)	7.748	7.541	0.486	0.500	0.014	4.117	3.631	0.138	2.334	4.228

deoxyribonucleosides and NRTIs is 0.242 eV. Among the deoxyribonucleosides, the maximum relaxation is found in the case of dC (0.348 eV), while among the analogues FTC (0.477 eV) has the maximum relaxation. We note that the adiabatic IP is useful in the analysis of mechanisms such as charge hopping and delocalization in DNA components, during phenomena such as photo-oxidation. For instance, the maximum relaxation, which occurs in the cation of dC

and its analogue, is due to extensive delocalization in the base part of these molecules, as was explained earlier in the discussion on the structural properties.

The experimental determination of the electron affinities (EA) for chemical systems such as drugs and biomolecules is a challenge. To the best of our knowledge, there are no available experimental electron affinity values for deoxyribonucleosides and NRTIs. Hence, theoretical calculations [61] of the EAs are particularly useful, as the EAs are essential not only for evaluating the reactivity descriptors, but also for explaining phenomena such as donor-acceptor interactions [62].

The most commonly employed method for the theoretical determination of EAs is DFT. It can be applied to a larger range of atoms and molecules [63] than any other ab initio method currently in use. In addition to the conventional ab initio methods (SCF, CI, MPn, and CC), other theoretical methods for predicting EAs include Green's function methods [64], those based on the extended Koopmans' theorem [65], electron propagator approximations [66], and calculations from known experimental half-wave reduction potentials [67]. EAs obtained with DFT methods are fairly accurate (within 0.2 eV or less) in most cases [63].

We note that the experimental estimates of the EAs for the DNA bases are sometimes inconsistent [10, 62]: while some reported values are positive, others give the same value as negative. Our computed values for the EA of the DNA bases, reported in an earlier work [59], are consistent with the data from electron capture experiments [62].

A measure of understanding of the EAs may be obtained by an examination of the dipole moment values, given in Table 2; and the geometry relaxations upon anion formation, given in Table 1. We note that our computed dipole moments for the DNA bases are in better agreement with the experimental values than earlier theoretical calculations using B3LYP/DZP++[10]. Except abacavir (ABC), all the deoxyribonucleosides and analogues (NRTIs) have large dipole moments. Further, there is not much geometry relaxation upon anion formation, so that the difference between the vertical and adiabatic EA is small(seen in the negligible RMSD (0.042 eV)). Hence, the large EA in these molecules may be attributed to the formation of dipole-bound anions [10, 68, 69]. On the other hand, in the case of AZT, though the dipole moment is large, there is a large geometry relaxation around the azide group upon anion formation. This is also reflected in the large difference (0.497 eV) between the vertical and adiabatic EA. Hence, in this case, the large value of the EA may be attributed to the accommodation of the electron over the entire molecule.

The presence of the deoxyribose would also be expected to alter the values of the EA of the deoxyribonucleosides or their analogues, as compared to the base. We have found an increase in the EA of the deoxyribonucleosides (except for Guanine) over the isolated base counterparts. A similar trend has also been obtained by other investigators using B3LYP/DZP++[10]. The adiabatic EA of all the NRTIs (except dC analogues) have been found to be higher than the corresponding bases.

Global chemical reactivity descriptors

A quantitative analysis of the reactivity of the molecule is obtained by the determination of the global reactivity descriptors, for which the accurately evaluated vertical ionization potential and electron affinity may be used. The values of the global reactivity descriptors, calculated for each of the drug molecules and for the deoxyribonucleosides, using the vertical IP and EA, are given in Table 2. Electronegativity (χ), which is the negative of the chemical potential (μ), is a measure of the tendency of the molecule to attract electrons. The dA analogue, ddI, has a higher electonegativity (4.105 eV) than dA (4.058 eV). For the dT analogues, d4T and AZT, the values are 4.266 eV and 4.191 eV, respectively, whereas for dT it is 4.246 eV. ABC, the dG analogue, has a value 3.621 eV, whereas its counterpart dG has a value 3.938 eV. The electronegativity of the dC analogues, viz. 3TC, ddC and FTC are 4.065 eV, 4.117 eV and 4.179 eV, respectively, whereas for dC it is 4.203 eV. Among the deoxyribonucleosides, the electronegativity decreases in the order dT>dC>dA>dG.

Hardness is a direct measure of the stability of a molecule, and softness provides a measure of its reactivity. The computed chemical hardness (η) for the NRTIs ranges from 3.051 eV to 3.759 eV, whereas for the corresponding deoxyribonucleosides it ranges between 3.508 eV and 3.734 eV. The hardness values of the NRTIs, with the exception of d4T among the dT analogues, and ddI among the dA analogues, are found to be lower than the values for the corresponding nuleosides. This indicates that these drugs have a higher tendency to undergo phosphorylation compared to their natural deoxyribonucleosides, enabling them to successfully get incorporated into the viral DNA, and causing chain termination. Thus, this explains why these drugs are effective in drug action. We note that among the dC analogues, ddC has the maximum hardness (η=3.631 eV). This is in line with the experimental finding [72] that ddC is the least potent among the dC analogues.

Normally, a combination of two or three drugs is often administered clinically. However, certain drugs are not administered together, for example, 3TC and ddC. The reason for this can be understood from the hardness and softness parameters of these drugs. Both these drugs compete for the attachment to the phosphate group, and as 3TC has a hardness value (η=3.562) lower than that of ddC (η=3.631 eV), 3TC will attach itself to the phosphorous of the phosphate group, preventing the attachment of ddC during phosphorylation. Hence, for both these drugs to be effective, 3TC and ddC

should not be administered together, a fact that is part of clinical wisdom. Our study also indicates that among the dT analogues, d4T is more stable (η=3.759 eV) than AZT (η= 3.631 eV), and has a stability comparable to that of dT (η= 3.734 eV). Our results explain the prevention of the simultaneous use of AZT along with d4T, as the former can inhibit the intracellular phosphorylation of d4T. Among the NRTIs, ABC is found to have a hardness value (η=3.051 eV) which differs the maximum (0.457 eV) from its corresponding nucleoside, dG (η=3.508 eV).

Local chemical reactivity descriptors

One of the quantum chemical tools widely used to probe the reactive sites in a molecule is the Fukui function [20, 31]. In order to probe the reactivity toward monophosphorylation (Fig. 3) of various NRTIs and the deoxyribonucleosides, the condensed-to-oxygen-atom Fukui function f_k^- was evaluated at the primary hydroxyl group of the $C_{5'}$ site of these molecules (Table 3). f_k^-, indicates the decrease in negative charge from the site k(oxygen atom), upon the removal of one electron from the molecule. The greater the magnitude of f_k^-, the greater the loss in charge on the oxygen atom and consequently, the greater the increase in charge on the phosphorous, i.e., there is charge density transfer from the oxygen to the phosphorous of the phosphate group, and hence the molecule (NRTI or its analogue) has undergone monophosphorylation.

We note that the condensed Fukui function is a local reactivity descriptor and can be used only for comparing the reactive atomic centers within the same molecule. As mentioned earlier, the local softness indices $s(\vec{r})$ are closely related to f_k^-, for comparing the reactivity of sites on different molecules. It is clear from Table 3, that except for AZT and 3TC, for all the other NRTIs, the condensed-to-oxygen-atom local softness value is greater than for the corresponding deoxyribonucleoside. We note also that the trend in the local softness of the molecules is the same as that of the Fukui function. In the case of the deoxyribonucleosides, upon removal of an electron, the decrease in negative charge on the deoxyribose moiety is shared by the two hydroxyl groups present at C_3' and C_5' positions. On the other hand in the analogues (NRTIs), the sugar moiety has only one hydroxyl group at C_5' position. Hence, in the NRTIs, upon removal of an electron, the decrease in the negative charge occurs from the C_5' hydroxyl oxygen. So, the loss in negative charge from the C_5' hydroxyl oxygen is larger in the NRTIs than in the corresponding deoxyribonucleosides, thus rendering the drugs more active for monophosphorylation. This is in consonance with the general understanding in the literature [74], obtained through various experiments, that monophosphorylation is the crucial step in the phosphorylation of the NRTIs.

For the drugs AZT and 3TC, however, it would appear that monophosphorylation is not the rate-determining step in the phosphorylation reactions. This may be understood as follows: For AZT, the smaller value of the condensed-to-oxygen-atom Fukui function for the C_5' hydroxyl oxygen (f_k^-=0.015) is due to the presence of the azide group at the C_3' position (the terminal nitrogens of the azide group (N=N=N-) have f_k^- values (0.113 and=0.069)). This indicates that the maximum decrease in negative charge in the deoxyribose moiety is from the azide group and not from the C_5' hydroxyl oxygen. Similarly, in 3TC, the smaller value of f_k^- (= 0.029) on the C_5' hydroxyl oxygen is due to the presence of a sulphur atom in the deoxyribose moiety at the 3′ position (f_k^-=0.141).

Table 3 indicates the order of effectiveness of the different drugs within the same category. We find d4T and ddC to be the most effective among their respective categories, in contradiction to the experimental finding that they are least effective in their respective categories. Once again, this seems to indicate that for AZT and 3TC, monophosphorylation is not the rate-determining step in the phosphorylation reactions. Further work, on the di-and tri-phosphorylation

Table 3 Calculated electronic population q_k and the local chemical reactivity descriptors, viz., Fukui function (f_k^-)for electrophilic attack, local softness ($s(\vec{r})$) and philicity ($\omega(\vec{r})$), at the 5′ O atom, for the deoxyribonucleosides and their analogues (NRTIs)

Deoxyribonucleosides/ analogues (NRTIs)	$q_k(N)$	$q_k(N-1)$	$f_k^- = \lvert q_k(N) - q_k(N-1)\rvert$	$s(\vec{r})$	$\omega(\vec{r})$
dA	−0.364	−0.360	0.004	0.0006	0.0093
ddI	−0.389	−0.300	0.089	0.0124	0.2081
dT	−0.368	−0.328	0.040	0.0054	0.0966
d4T	−0.87	−0.319	0.068	0.0090	0.1646
AZT	−0.379	−0.364	0.015	0.0020	0.0361
dG	−0.366	−0.357	0.009	0.0013	0.0200
ABC	−0.373	−0.352	0.021	0.0034	0.0451
dC	−0.369	−0.327	0.042	0.0057	0.1009
FTC	−0.370	−0.319	0.051	0.0071	0.1251
3TC	−0.382	−0.353	0.029	0.0041	0.0673
ddC	−0.370	−0.285	0.085	0.0117	0.1984

reactions, would be required to clarify these issues. In addition to the studied descriptors, several other factors such as the nature of the target, concentration of the drugs at the active sites and their dependence on pharmacokinetic factors such as adsorption, distribution, metabolism and excretion would also need to be taken into account.

Conclusions

We have carried out detailed first-principles density functional calculations of the structures, energetics, ionization potentials, electron affinities and various global chemical reactivity descriptors of the NRTI drug molecules and their respective deoxyribonucleosides, in both neutral and charged states.

The bond lengths and bond angles determined by geometry optimization are in good agreement with the experimental results available in the literature for several of the drugs, such as 3TC, d4T, ddC and AZT, giving confidence in the ability of DFT to accurately describe this class of systems. The geometry-optimized structures of the deoxyribonucleosides and their analogues show that the geometrical variation from the neutral structure, is greater in the cations, than in the anions, except in the case of AZT. In the pyrimidine-based nucleosides and their analogues, there is alternate bond elongation and bond shortening in the base bonds on cation formation, suggesting extensive delocalization in the base moiety of the cations. The glycosidic bond becomes weaker in the cation, which implies that exposure to an oxidizing agent or radiation may cause its cleavage; and, it becomes stronger in the anion. There is no significant variation in the sugar moiety of the anion, implying that the excess charge resides on the nucleic acid bases of these molecules.

The presence of the sugar has a strong effect on the energetics of the ionization of the base in both deoxyribonucleosides and NRTIs, and their computed vertical and adiabatic IPs are lower than in the corresponding bases. On the other hand, the EAs of these molecules are found to be higher than those of their corresponding bases.

Using global reactivity parameters, the reactivity of the drug molecules toward phosphorylation is compared with that of the corresponding deoxyribonucleosides, and is found to be greater than that of the latter in all cases except d4T and ddI. Importantly, this explains the effectiveness of the drug action in the chain termination of the viral DNA. Using hardness and softness parameters, we are also able to understand how certain drugs compete with each other for phosphorylation, thus rendering one of them ineffective. This helps to explain the clinical practice of avoiding the simultaneous administration of these drugs. Our study using local reactivity parameters confirms, for all the NRTIs except AZT and 3TC, the accepted wisdom that monophosphorylation is the crucial step in the phosphorylation reaction in DNA nucleotide synthesis. Inspite of our ability to describe the activity of most of the NRTIs from just the global and local chemical descriptors, clearly several other factors would be expected to play an important role in such complex biochemical processes. Hence, a more complete study in the future would explain the role of factors such as the nature of the target, the concentration of drugs at the active site etc., which in turn would depend on pharmacokinetic factors such as adsorption, distribution, metabolism and excretion.

Acknowledgements This work was supported by DAE-BRNS grant (sanction no. 2010/37C/58/BRNS) and was possible due to the facilities, and help from the staff, of the BARC-Mumbai and IUAC-New Delhi computer centre.

References

1. Varatharajan L, Thomas SA (2009) The transport of anti-HIV drugs across blood-CNS inter- faces: summary of current knowledge and recommendations for further research. Antiviral Res 82: A99–A109
2. Arias LM (2008) Mechanisms of resistance to nucleoside analogue inhibitors of HIV-1 reverse transcriptase. Virus Res 134:124–146
3. Back DJ, Burger DM, Flexner CW, Gerber JG (2005) The pharmacology of antiretroviral nucleoside and nucleotide reverse transcriptase inhibitors: implications for once-daily dosing. J Acquir Immune Defic Syndr 39(suppl 1):S1–23
4. Sarafianos SG, Marchand B, Das K, Himmel DM, Parniak MA, Hughes SH, Arnold E (2009) Structure and function of HIV-1 reverse transcriptase: molecular mechanisms of polymerization and inhibition. J Mol Biol 385:693–713
5. Orlov VM, Smirnov AN, Varshavsky Ya M (1976) Ionization potentials and electron-donor ability of nucleic acids bases and their analogues. Tetrahedron Lett 48:4377–4378
6. Hendricks JH, Lyapustina SA, de Clercq HL, Snodgrass JT, Bowen KH (1996) Dipole-bound, nucleic acid base anions studied via negative ion photoelectron spectroscopy. J Chem Phys 104:7788–7791
7. Close DM (2004) Calculation of the ionization potentials of the DNA bases in aqueous medium. J Phys Chem A 108:10376–10379
8. Yu C, O'Donnell TJ, LeBteton PR (1981) Ultraviolet photoelectron studies of volatile nucleoside models. Vertical ionization potential measurements of methylated uridine, thymidine, cytidine, and adenosine. J Phys Chem 85:3851–3855
9. Pluharova E, Jungwirth P, Bradforth SE, Slavicek P (2011) Ionization of purine tautomers in nucleobases, nucleosides, and nucleotides: from the gas phase to the aqueous environment. J Phys Chem B 115:1294–1305
10. Richardson NA, Gu J, Wang S, Xie Y, Schaefer HF (2004) DNA nucleosides and their radical anions: molecular structures and electron affinities. J Am Chem Soc 126:4404–4411
11. Palafox MA, Iza N, de la Fuente M, Navarro R (2009) Simulation of the first hydration shell of nucleosides D4T and thymidine: structures obtained using MP2 and DFT methods. J Phys Chem B 113:2458–2476
12. Yekeler H (2004) Preferred conformations of some pyrimidine nucleoside reverse transcriptase inhibitors (NRTIs). J Mol Struct (Theochem) 684:223–230

13. Pereira BG, Vianna-Soares CD, Righi A, Pinheiro MVB, Flores MZS, Bezerra EM, Freire VN, Lemos V, Caetano EWS, Cavada BS (2007) Identification of lamivudine conformers by Raman scattering measurements and quantum chemical calculations. J Pharma Biomed Anal 43:1885–1889
14. Fidanza NG, Suvire FD, Sosa GL, Lobayan RM, Enriz RD, Peruchena NM (2001) A search for C-H…O type hydrogen bonds in Lamivudine (3TC). An exploratory conformational and electronic analysis. J Mol Struct(Theochem) 543:185–193
15. Fidanza NG, Sosa GL, Lobayan RM, Peruchena NM (2005) Topological analysis of the electronic charge density in nucleoside analogues derivatives of the AZT. Effects of XH/O and XH/F intramolecular H-bonds. J Mol Struct(Theochem) 722:65–78
16. Carvalho ATP, Fernandes PA, Ramos MJ (2007) The excision mechanism in reverse transcriptase: pyrophosphate leaving and fingers opening are uncoupled events with the analogues AZT and d4T. J Phys Chem B 111:12032–12039
17. Parr RG, Yang W (1989) Density-functional theory of atoms and molecules. Oxford University Press, New York
18. Parr RG, Yang WT (1995) Density functional theory of electronic structure of the molecules. Annu Rev Phys Chem 46:701–728
19. Kohn W, Becke AD, Parr RG (1996) Density functional theory of electronic structure. J Phys Chem 100:12974–12980
20. Geerlings P, De Proft F, Langenaeker W (2003) Conceptual density functional theory. Chem Rev 103:1793–1874
21. Geerlings P, De Proft F (2008) Conceptual DFT: the chemical relevance of higher response functions. Phys Chem Chem Phys 10:3028–3042
22. Ayers PW, Anderson JSM, Bartolotti LJ (2005) Perturbative perspectives on the chemical reaction prediction problem. Int J Quantum Chem 101:520–534
23. Chermette H (1999) Chemical reactivity indexes in density functional theory. J Comput Chem 20:129–154, and ref. cited therein
24. Mulliken RS (1934) A New Electroaffinity Scale; Together with Data on Valence States and on Valence Ionization Potentials and Electron Affinities. J Chem Phys 2:782–793
25. Mulliken RS (1935) Electronic Structure of the Molecules XI. Electroaffinity, Molecular Orbitals and Moments. J Chem Phys 3:573–585
26. Parr RG, Donnelly RA, Levy M, Palke WE (1978) Electronegativity: the density functional viewpoint. J Chem Phys 68:3801–3807
27. Pearson RG (1986) Absolute electronegativity and hardness correlated with molecular orbital theory. Proc Nati Acad Sci USA 83:8440–8441
28. Yang W, Parr RG (1985) Hardness, softness, and the fukui function in the electronic theory of metals and catalysis. Proc Nati Acad Sci USA 82:6723–6726
29. Parr RG, Lv S, Liu S (1999) Electrophilicity Index. J Am Chem Soc 121:1922–1924
30. Chattaraj PK, Sarkar U, Roy DR (2006) Electrophilicity index. Chem Rev 106:2065–2091
31. Yang W, Mortier WJ (1986) The use of global and local molecular parameters for the analysis of the gas-phase basicity of amines. J Am Chem Soc 108:5708–5711
32. Hohenberg P, Kohn W (1964) Inhomogeneous Electron Gas. Phys Rev 136:3864–3871
33. Kohn W, Sham LJ (1965) Self-Consistent Equations Including Exchange and Correlation Effects. Phys Rev 140:A1133–A1138
34. Ayers P W, Yang W (2003) "Density functional theory", in computational medicinal chemistry for drug discovery. Bultinck P, De Winter H, Langenaeker W, Tollenaere J, (Eds) Dekker, New York, pp 571
35. Ceperley DM, Alder BJ (1980) Ground state of the electron gas by a stochastic method. Phys Rev Lett 45:566–569
36. Troullier N, Martins JL (1991) Efficient pseudopotentials for plane-wave calculations. Phys Rev B 43:1993–2006
37. Ramaniah LM, Bernasconi M, Parrinello M (1998) Density-functional study of hydration of sodium in water clusters. J Chem Phys 109:6839–6843
38. Ramaniah LM, Bernasconi M, Parrinello M (1999) Ab initio molecular-dynamics simulation of K^+ solvation in water. J Chem Phys 111: 587–1591
39. Ramaniah LM, Boero M, Laghate M (2004) Tantalum-fullerene clusters: a first-principles study of static properties and dynamical behavior. Phys Rev B 70:o35411–o35424
40. Ramaniah LM, Boero N (2006) Structural, electronic, and optical properties of the diindenoperylene molecule from firstprinciples density-functional theory. Phys Rev A 74:o42505–o42509
41. Ramaniah LM, Chakrabarti A, Kshirsagar RJ, Kamal C, Banerjee A (2011) Density functional study of α-amino acids: structural, energetic and vibrational properties. Molecular Physics 109:875–892
42. Barnett RN, Landman U (1993) Born-Oppenheimer molecular-dynamics simulations of finite systems: and dynamics of $(H_2O)_2$. Phys Rev B 48:2081–2097
43. Tuckerman ME, Martyna GJ (2005) Efficient Evaluation of Non-local Pseudopotentials via Euler Exponential Spline Interpolation. Chem Phys Chem 6:1827–1835
44. Tuckerman ME, Martyna GJ (2002) A new reciprocal space based treatment of long range interactions on surfaces. J Chem Phys 116:5351–5362
45. Hutter J, Luthi Al P, Parrinello M (1993) Electronic structure optimization in plane-wave-based density functional calculations by direct inversion in the iterative subspace. Comput Mater Sci 2:244–248
46. Car R, Parrinello M (1985) Unified Approach for Molecular Dynamics and Density-Functional Theory. Phys Rev Lett 55:2471–2474
47. CPMD, Copyright IBM Corp.1990-2004,Copyright Max-Planck-Institut für Festkörperforschung, Stuttgart, 1997 - 2001.
48. Becke AD (1988) Density-functional exchange-energy approximation with correct asymptotic behavior. Phys Rev A 38:3098–3100
49. Lee C, Yang W, Parr RG (1988) Development of the Colle-Salvetti correlation-energy formula into a functional of the electron density. Phys Rev B 37:785–789
50. Harte WE, Starrett JE, Martin JC, Mansuri MM (1991) Structural studies of the anti-HIV agent 2′, 3′-didehydro-2′, 3′-dideoxythymidine (D4T). Biochem Biophys Res Commun 175:298–304
51. Birnbaum GI, Lin TS, Prusoff WH (1988) Unusual structural features of 2′, 3′-Dideoxycytidine, an inhibitor of the HIV (AIDS) virus. Biochem Biophys Res Commun 151:608–614
52. Dyer I, Low JN, Tollin P, Wilson HR, Howie RA (1988) Structure of 3′-Azido-3′- deoxythymidine, AZT. Acta Cryst C 44:767–769
53. Birnbaum GI, Giziewicz J, Gabe EJ, Lin TS, Prusoff WH (1987) Structure and conformation of 3′-azido-3′ -deoxythymidine (AZT), an inhibitor of the HIV (AIDS) virus. Can J Chem 65:2135–3139
54. Sato T (1984) Structure of 2′-deoxyadenosine, $C_{10}H_{13}N_5O_3$. Acta Cryst C 40:880–882
55. Young DW, Wilson HR (1975) The crystal and molecular structure of 2′-deoxycytidine. Acta Cryst B 31:961–965
56. Young DW, Tollin P, Wilson HR (1969) The crystal and molecular structure of thymidine. Acta Cryst B 25:1423–1432
57. Candeias LP, Steenken S (1992) Ionization of purine nucleosides and nucleotides and their components by 193-nm laser photolysis in aqueous solution: model studies for oxidative damage of DNA. J Am Chem Soc 114:699–704
58. Slavicek P, Winter B, Faubel M, Bradforth SE, Jungwirth P (2009) Ionization energies of aqueous nucleic acids: photoelectron spectroscopy of pyrimidine nucleosides and ab initio calculations. J Am Chem Soc 131:6460–6467
59. Kumar V, Jain G, Kishor S, Ramaniah LM (2011) Chemical reactivity analysis of some alkylating drug molecules: a density functional theory approach. Comput Theoret Chem 968:18–25

60. Kishor S, Dhayal SS, Mathur M, Ramaniah LM (2008) Structural and energetic properties of α-amino acids: a first principles density functional study. Mol Phys 106:2289–2300
61. Compton R N (1997) Atomic negative ions, In: Esaulov D (Ed.) Negative ions, Cambridge Press, and references therein
62. Chen ECM, Chen ESD, Wentworth WE (1990) The role of electron donors and acceptors in base stacking in DNA and RNA. Biochem Biophys Res Commu 171:97–101
63. Rienstra-Kiracofe JC, Tschumper GS, Schaefer HF, Nandi S, Ellison GB (2002) Atomic and molecular electron affinities: photoelectron experiments and theoretical computations. Chem Rev 102:231–282
64. Ohno M, Zakrzewski VG, Ortiz JV, Niessen WV (1997) Theoretical study of the valence ionization energies and electron affinities of linear C_{2n+1}(n=1–6) clusters. J Chem Phys 106:3258–3269
65. Cioslowski J, Piskorz P, Liu G (1997) Ionization potentials and electron affinities from the extended Koopmans' theorem applied to energy-derivative density matrices: the EKTMPn and EKTQ-CISD methods. J Chem Phys 107:6804–6811
66. Ortiz JV (1998) Electron detachment energies of closed-shell anions calculated with a renormalized electron propagator. Chem phys Lett 296:494–498
67. Chen ES, Chen ECM, Sane N, Talley L, Kozanecki N, Shulze S (1999) Classification of organic molecules to obtain electron affinities from half wave reduction potentials: the aromatic hydrocarbons. Chem Phys 110:9319–9329
68. Simons J, Jordan KD (1987) Ab initio electronic structure of anions. Chem Rev 87:535–555
69. Li X, Cai Z, Sevilla MD (2002) DFT calculations of the electron affinities of nucleic acid bases: dealing with negative electron affinities. J Phys Chem 106:1596–1603
70. Silverton QFR, Haugwitz RD, Todaro LJ (1988) Structures of two dideoxynueleosides: 2′, 3′-dideoxyadenosine and 2′, 3′-dideoxyeytidine. Acta Cryst C 44:321–324
71. Crespo-Hernandez CE, Close DM, Gorb L, Leszczynski J (2007) Determination of redox potentials for the Watson-Crick base pairs, DNA nucleosides, and relevant nucleoside analogues. J Phys Chem B 111:5386–5395
72. Goldschmidt RH, Dong BJ (2002) Treatment of AIDS and HIV-related conditions 2002: antiretroviral therapy. JAm Board Med Family (Antiretroviral Therapy) 15:319–331
73. Guckian KM, Schweitzer BA, Ren RX, Sheils CJ, Tahmassebi DC, Kool ET (2000) Factors contributing to aromatic stacking in water: evaluation in the context of DNA. J Am Chem Soc 122:2213–2222.
74. Cihlar T, Ray AS (2010) Nucleoside and nucleotide HIV reverse transcriptase inhibitors: 25 years after Zidovudine. Antiviral Res 85:39–58